POLISH POLAR RESEARCH
vol. 39, no. 1, pp. 51–75, 2018 doi: 10.24425/118738

Palaeomagnetism of metacarbonates and fracture fills of Kongsfjorden islands (western Spitsbergen): Towards a better understanding of late- to post-Caledonian tectonic rotations

Krzysztof MICHALSKI

Instytut Geofizyki, Polska Akademia Nauk,
ul. Księcia Janusza 64, 01-452 Warszawa, Poland
<krzysztof.michalski@igf.edu.pl>

Abstract: A total number of 156 palaeomagnetic specimens of metacarbonates from 9 sites in Blomstrandhalvøya and Lovénøyane (Kongsfjorden, western Spitsbergen) and an additional 77 specimens of unmetamorphosed sediments infilling fractures (4 sites) within the Caledonian metamorphic basement of Blomstrandhalvøya were demagnetized. No relicts of pre-metamorphic magnetization were identified. The Natural Remanent Magnetization (NRM) pattern of metacarbonates is dominated by Caledonian (*sensu lato*) – Svalbardian and Late Mesozoic/Cenozoic secondary magnetic overprints carried by the pyrrhotite and magnetite/maghemite phases, respectively. The NRM of unmetamorphosed sediments infilling the karstic/tectonic fractures is dominated by hematite carrier. It revealed three stages of magnetization: Caledonian *sensu lato*, Carboniferous and Late Mesozoic/Cenozoic, which can be related to their initial fracturing, karstification and sedimentation or reactivation. As the majority of the palaeopoles calculated for the Kongsfjorden sites fit the 430 – 0 Ma sector of Laurussia reference path in an *in situ* orientation these results support the hypothesis that Blomstrandhalvøya and Lovénøyane escaped main Eurekan deformations. The potential rotation of the Kongsfjorden basement by any west dipping listric fault activity rotating the succession accompanying the opening of North Atlantic Ocean was not documented by the palaeomagnetic data presented here.

Key words: Arctic, Svalbard, metamorphic Caledonian basement, Eurekan deformations, West Spitsbergen Thrust and Fold Belt, palaeomagnetism.

Introduction

The Caledonian basement of Western Spitsbergen, which constitutes a part of the so called Central Caledonian Terrane of Svalbard (Harland and Wright 1979), has been subjected to a number of late- and post-Caledonian tectonic and

tectono-thermal events. These events include a Late Devonian Svalbardian phase (*e.g.*, Manby and Lyberis 1992; Bergh *et al*. 2011), Cretaceous extension and injection of dolerites (*e.g.*, Nejbert *et al*. 2011; Polteau *et al*. 2016) and Cenozoic extension related to the opening of the North Atlantic Ocean which in Western Caledonian Terrane was accompanied by listric faulting of the basement (Burzyński *et al*. 2017; Michalski *et al*. 2017). The extent to which the Eurekan (*sensu lato*) intracontinental fold and thrust belt deformation of Western Spitsbergen (*e.g.*, Lyberis and Manby 1993; Maher *et al*. 1995; Bergh *et al*. 1997; Braathen *et al*. 1999; Leever *et al*. 2011; Piepjohn *et al*. 2016) has affected this block, is still insufficiently recognized.

The focus here is to determine the extent to which these deformation events have influenced the palaeomagnetic features and the geometry of the metamorphosed successions. To this end, the metacarbonates and post-Caledonian sedimentary fills of tectonic and karstic fractures found on Blomstrandhalvøya and Lovénøyane of Kongsfjorden (Fig. 1), are targeted for the palaeomagnetic investigations. The experiments conducted on both rock types include the detailed recognition of their Natural Remanent Magnetization (NRM) patterns and the identification of any pre-, syn- and post-Caledonian NRM components. As it has been established already that Central Caledonian Terrane constituted a part of the Baltica plate, at least from Silurian time (Szlachta *et al*. 2008; Michalski *et al*. 2012), it is important to determine whether the metacarbonates in the study areas retain any relicts of a pre-Caledonian (primary?) palaeomagnetic record. By comparing any syn- and post-Caledonian palaeomagnetic components found with the Baltica reference Apparent Polar Wander Path (APWP), it should be possible to evaluate the age, nature and scale of any potential tectonic rotations that have affected the investigated metamorphic block. In addition, the palaeomagnetic study of the fracture infillings presents a unique opportunity for establishing the timing of formation of the initial fractures and their subsequent reactivation.

In each of the palaeomagnetic sites, low field Anisotropy of Magnetic Susceptibility (AMS) ellipsoid was monitored to exclude those NRM components which could be tectonically modified. The AMS results are presented in the Supplementary material.

Geological setting

The metamorphic basement of Blomstrandhalvøya and Lovénøyane consists of inhomogeneous massive or laminated marbles containing variable quantities of graphite and dolomite (Thiedig *et al*. 2001). The whole metamorphosed succession cropping-out on the Kongsfjorden islands belongs to the upper part of the Generalfjella Formation, of the Krossfjorden Group (Gee and Hjelle 1966; Hjelle 1979). These marbles in the study areas are unconformably overlain by narrow

faulted slices of Lower Devonian (?) marble breccias, that are covered by red sandstones and conglomerates of the Red Bay Group (Friend 1961; Thiedig *et al*. 2001). The Blomstrandhalvøya marbles are karstified in numerous locations (Fig. 1) and most host fills of red beds of presumed Old Red Sandstone age. Some, almost pure quartz sandstone fills have been shown to be of Middle to Late Carboniferous age on the basis of conodont remains (Buggish *et al*. 1994).

The marbles exhibit three phases of folding and low-grade metamorphism (Kempe *et al*. 1997). The large-scale Caledonian NNE-SSW to NNW-SSE trending F1 folds are associated with the main metamorphic event and are recumbent to almost flat-lying the axial-plane S1 foliation, which is widely characterized by high shear strains, is inclined to the east. The F1 folds are refolded by decametric scale F2 folds that are associated with a steep, east-dipping fracture-like S2 cleavage (Manby, personal communication). A number of these folds are cut by out-of-syncline east dipping contractional faults that are often characterized by red-stained breccias. The F3 folds, where they are found, are more crenulation--kink like structures associated with NW-SE and NE-SW steep dipping conjugate fracture sets cutting the main S1 foliation (Manby, personal communication).

The pockets of Devonian red breccias, conglomerates and sandstones are in some cases affected by west-directed contractional faults, while in other sites east and west inclined normal faults are dominant. In both fault zone types, the infilling sediments may be folded and show some weak tectonic fabric although in the case of the better exposed eastern location the folded sediments are covered by totally undeformed red sedimentary breccia. The age of the faulting and deformation of the red sedimentary fills has been attributed to the either the Late Devonian Svalbardian or related to Eurekan West Spitsbergen Fold and Thrust Belt (WSFTB) deformation events, *e.g*., Thiedig and Manby (1992). Buggish *et al*. (1994) suggests, however, that the folding and thrusting of the red beds (Wood Bay Group) must have taken place before the karstification of the marbles, probably during the Svalbardian event as the Middle to Late Carboniferous karst sediments are virtually undeformed. According to Thiedig *et al*. (2001) and references therein, rocks exposed on Blomstrandhalvøya and Lovénøyane were unaffected by the main Eurekan deformation.

Material and methods

A total of 59 independently oriented palaeomagnetic samples of metacarbonates were collected from 9 sites situated in different locations on Blomstrandhalvøya (8 sites) and Lovénøyane (1 site) – see Fig. 1. A further 32 independently oriented palaeomagnetic samples were collected from 4 sites representing the undeformed red sandstones infilling the irregular fractures within metamorphic basement of Blomstrandhalvøya.

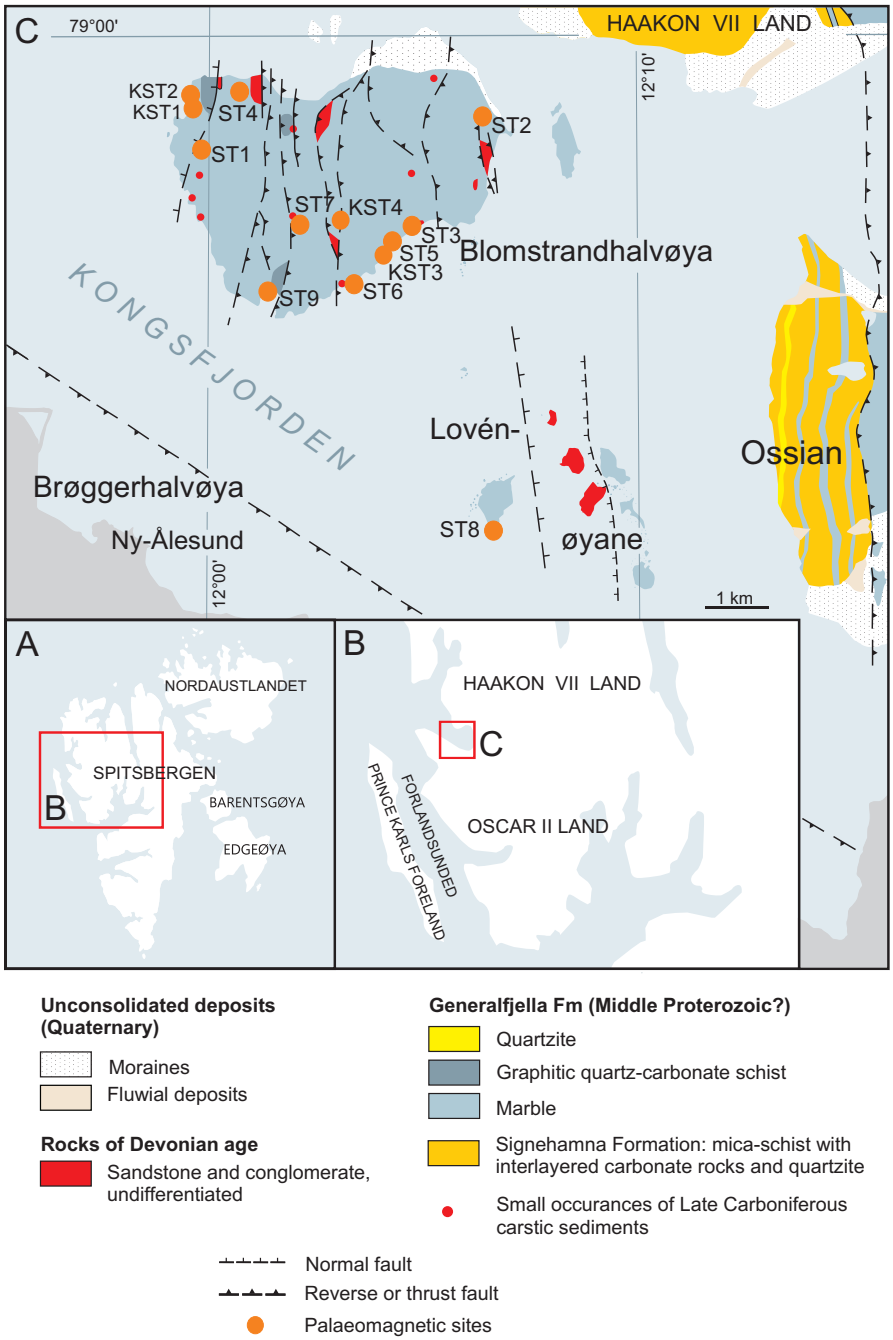

Fig. 1. Location of the study in Svalbard (**A**) and in Central Western Spitsbergen (**B**), as well as geological map of Blomstrandhalvøya and Lovénøyane (Kongsfjorden) modified after Hjelle *et al.* (1999) and Thiedig *et al.* (2001) (**C**); palaeomagnetic sampling sites are marked by orange dots.

To identify the ferromagnetic carriers and determinate the palaeomagnetic directions standard rock magnetic and palaeomagnetic procedures were used; for methods see Michalski *et al*. (2012, 2014).

The samples were subjected to the following rock – magnetic experiments: (i) Isothermal Remanent Magnetization (IRM) experiments were performed up to 3 mT using the MMPM–10 pulse magnetizer. Magnetization of the specimens was measured on the Superconducting Quantum Interface Device – SQUID (2G Enterprise model 755, USA) with a residual internal field of below 3nT and a noise level of about 5 μA/m; (ii) The parameters of the hysteresis loops (saturation magnetization – M_s; saturation remanence – M_{rs}; coercivity – H_c) as well as the coercive force (H_{cr}) were measured using a PMC MicroMag 2900 Series AGM VSM in maximum field 1T; and (iii) the three component IRM analyses (Lowrie 1990) were conducted using an MMPM-10 pulse magnetizer and SQUID. Thermal demagnetization was conducted in steps up to 680ºC in the MMTD1 (Magnetic Measurements thermal demagnetizer, Great Britain) furnace.

A total number of 233 cylindrical specimens (156 specimens of metacarbonates and 77 specimens of fractures infillings) were subjected to AMS and demagnetization procedures. In the course of the preliminary Alternating Field (AF)/thermal demagnetization experiments, the thermal method appeared to be the most effective for extracting the NRM components. All samples were thermally demagnetized in steps up to 680ºC in the MMTD1 furnace and, after each heating step, their residual magnetic field was measured using the SQUID. In the course of the demagnetization process the susceptibility of the specimens was controlled using the KLY-2 Kappa Bridge (Geophysica Brno, Czechoslovakia). The AMS of the specimens were measured on the AGICO MFK1–FA, susceptibility bridge. AMS ellipsoids were calculated using ANISOFT 42 software (Chadima and Jelinek 2009).

The palaeomagnetic components and the mean site directions were calculated using the REMASOFT 3.0 software (Chadima and Hrouda 2009), which employs the principal component analysis (PCA) after Kirschvink (1980) and Fisher (1953) statistics. The palaeomagnetic components were calculated on the orthogonal Zijderveld diagrams as a direction of best fit line to a minimum of three points, with a maximum Angular Standard Deviation (ASD) of 10º precision (80% of directions were defined with max. ASD = 8º, 50% – max. ASD = 6º). Only those samples with site means which passed the modified criteria of Van der Voo (1993) with values of $\kappa>10$ and $\alpha95<16^{\circ}$ and where the minimum number of independently oriented samples used for site mean calculation (N) equaled 3 were used for further tectonic and palaeogeographic interpretation. The tectonic corrections were applied using the SPHERISTAT 3.2.1. software. Palaeogeographic simulations were performed using the GMAP 2012 software. The reference palaeopole paths for Baltica and Laurentia were acquired from integral libraries of GMAP 2012 (Torsvik *et al*. 2012).

Results

Rock-magnetic experiments. — The IRM experiments revealed a prevalence of low to medium coercivity fractions in the metacarbonates, although some samples did not become saturated in the maximum applied 3T field indicating the presence of high coercivity phases (Fig. 2A). In all of the investigated fracture infillings the high coercivity grains were dominant (Fig. 2B). The preliminary coercivity estimations, determined from their IRM curves, were confirmed by the MicroMag measurements. The hysteresis loops and the remanent coercive force experiments (H_{cr}) on the metacarbonates confirmed the occurrence of low coercivity minerals (H_c<10 mT, H_{cr}~15mT; Fig. 3A and B). The high H_c>150 mT and H_{cr}>400 mT values determined for the fracture infilling sediments indicate, in contrast, the presence of high coercivity phases (Fig. 3C and D). Wasp-waisted shape of hysteresis loop in Fig. 3D suggests co-existence of high and low coercivity fractions in the sample (Dunlop and Özdemir 1997).

More precise estimations of the ferromagnetic content were based on the three component IRM analyses (Fig. 4). Most of the metacarbonates sites were found to be dominated by soft and medium fractions which saturated in the 400 mT field that were characterized by distinct maximum unblocking temperatures ($T_{ub\ max}$) in the 300–375ºC, 400–450ºC and 500–575ºC ranges (Fig. 4B–D). The 300–375ºC, range of temperatures approaches the $T_{ub\ max}$ of pyrrhotite (Dekkers 1989) which is a common phase found in the Hornsund (Michalski *et al*. 2012) and St. Jonsfjorden metacarbonate complexes (Michalski *et al*. 2014). Phases with $T_{ub\ max}$ values in the 400–450ºC range are more likely to be maghemite or titanomagnetite. The 500–575º range $T_{ub\ max}$ values reflects the presence of low-Ti

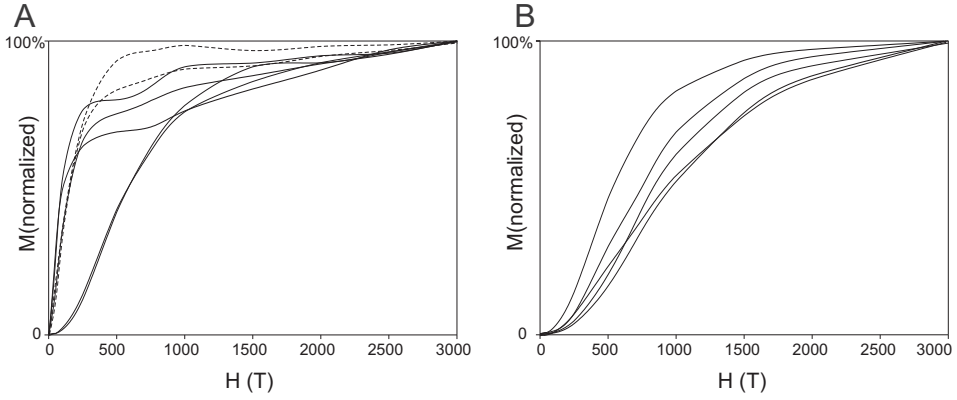

Fig. 2. Examples of IRM (Isothermal Remanent Magnetization) curves obtained for the metacarbonate samples (**A**) and red sediments infilling the karstic/tectonic fractures (**B**) from Blomstrandhalvøya and Lovénøyane (Kongsfjorden). Striped lines in diagram A represent samples from sites ST5 and ST8 in which the results of the three-component IRM acquisition experiments (Lowrie 1990) point to occurrence of pyrrhotite.

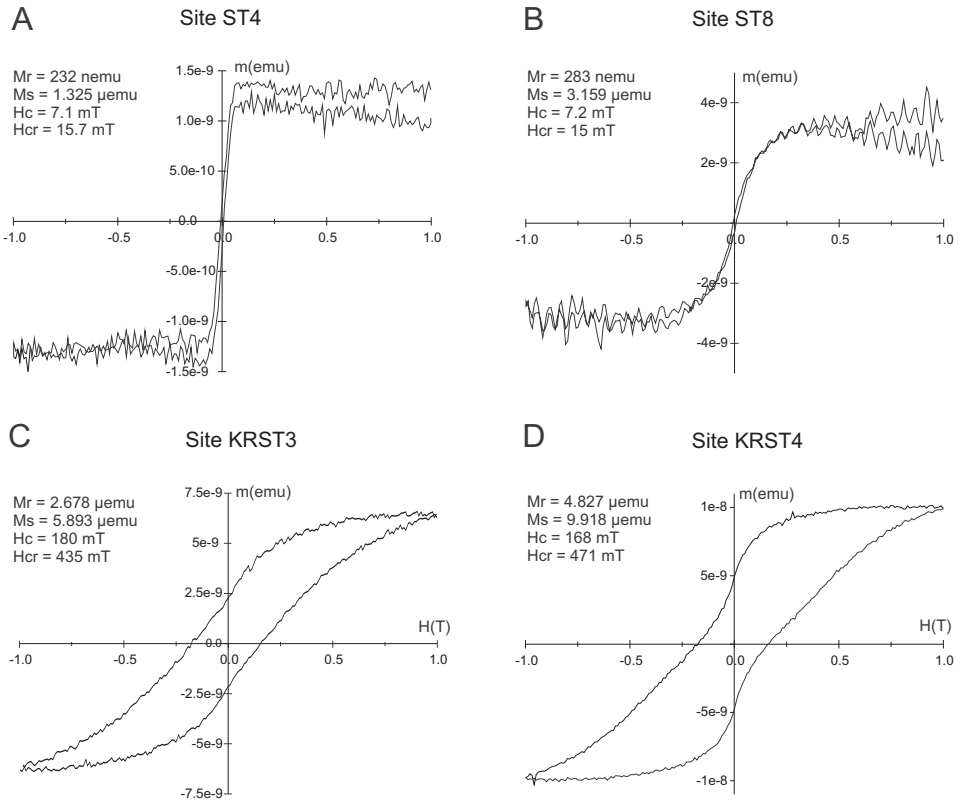

Fig. 3. Examples of hysteresis loops of metacarbonates (**A** and **B**) and red sediments infilling karstic/tectonic fractures (**C** and **D**) from Blomstrandhalvøya and Lovénøyane (Kongsfjorden).

magnetite (Dunlop and Özdemir 1997). The metacarbonate site ST2 represents an exception with a dominant high coercivity fraction that saturated above 400 mT up to 3T and possesses a distinct $T_{ub\ max}$ around 680ºC (Fig. 4A); values that correspond to those of hematite (Dunlop and Özdemir 1997). All of the sampled fracture fill sediments display, in contrast to the metacarbonates, a dominant high coercivity fraction with $T_{ub\ max}$ around 680–700ºC (Fig. 4E and F), that is a characteristic for hematite (Dunlop and Özdemir 1997).

Components of NRM. — The palaeomagnetic properties of the investigated metacarbonates and unmetamorphosed fractures fills differ. The initial NRM signal of the metacarbonates falls into the 5 10^{-6} – 8 10^{-4} A/m range. The fracture fills are characterized by NRM intensities from 5 10^{-6} A/m up to 1.5 10^{-2} A/m. The metacarbonate samples revealed very low susceptibility values

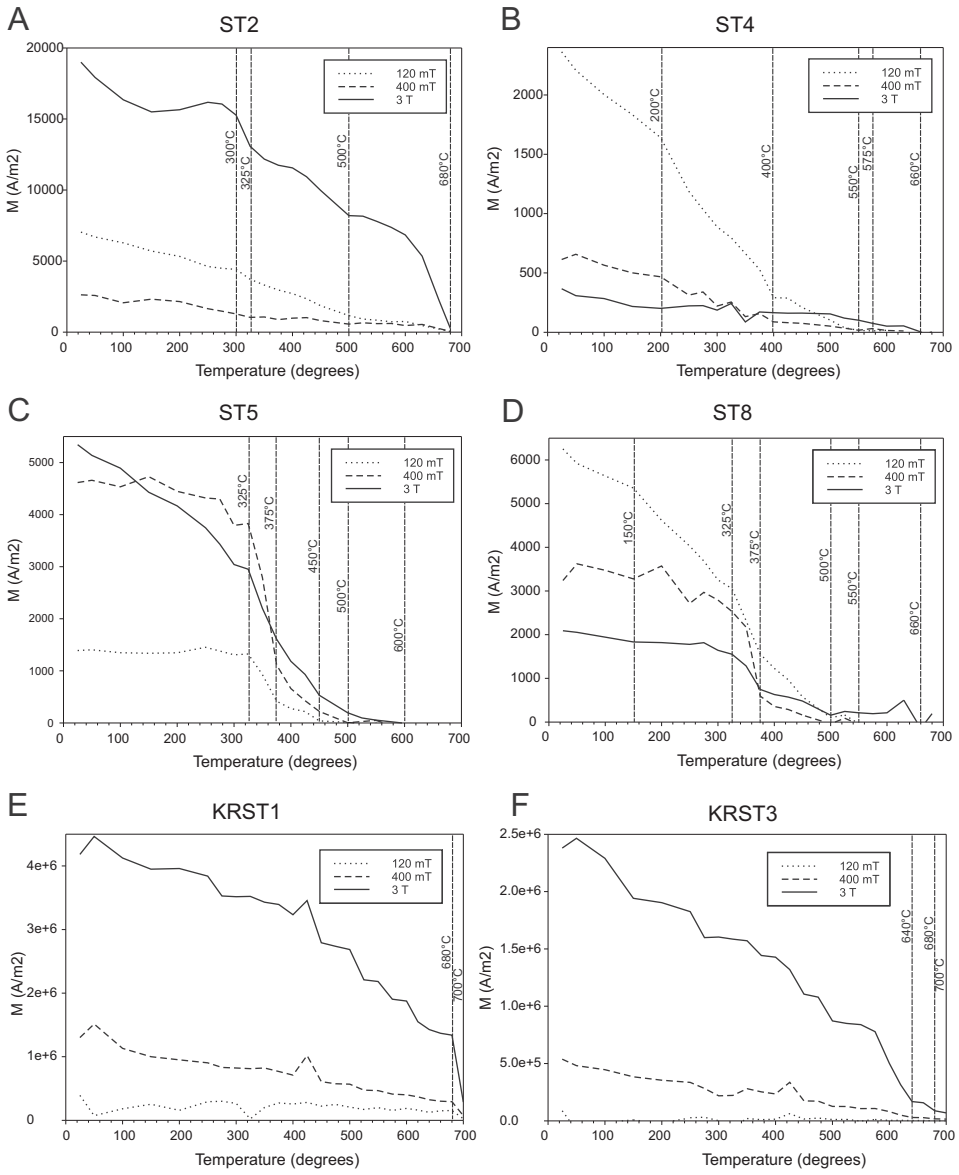

Fig. 4. Three-component IRM acquisition curves (Lowrie 1990) of the metacarbonates (**A**–**D**) and the red sediments of the karstic/tectonic fractures (**E** and **F**) from Kongsfjorden; lines represent ferromagnetic grains of different coercivity spectra: dotted lines indicate grains saturated up to 120 mT; dashed lines indicate those saturated between 120 and 400 mT; solid lines indicate those saturated between 400 mT and 3 T.

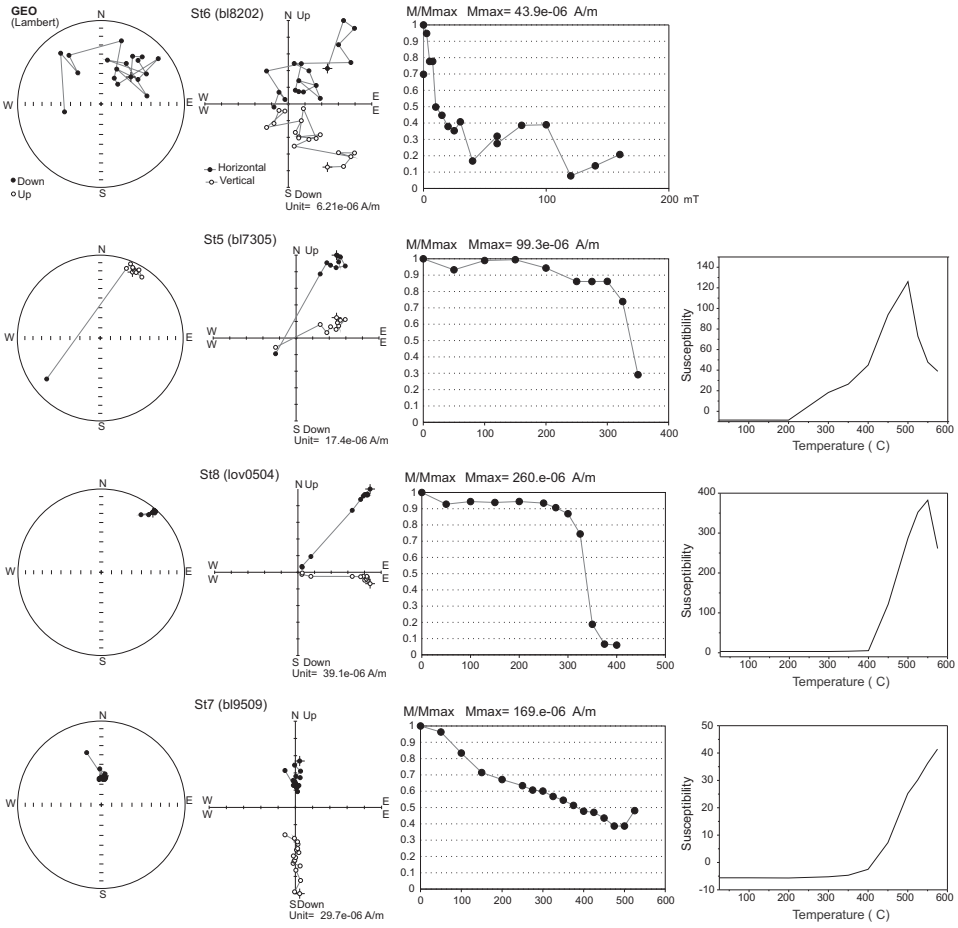

Fig. 5. Examples of AF and thermal demagnetization and susceptibility diagrams of the metacarbonates from Kongsfjorden; first diagrams (site ST6 – specimen bl8202) show example of not effective AF demagnetization; first column – equal area projections; second column – Zijderveld diagrams; third column – normalized intensity decay plots; fourth column – changes of susceptibility during thermal demagnetization procedures; projections are presented for *in situ* orientation; on equal area open symbols represent upper hemisphere and filled symbols represent lower hemisphere; on Zijderveld diagrams open symbols represent projections onto vertical planes and filled symbols denote projection onto horizontal plane.

from -10 10^{-6} SI (diamagnetic behavior) up to +10 10^{-6} SI. The unmetamorphosed fracture fills exhibited, on the other hand, higher susceptibility values up to +800 10^{-6} SI. In the course of the thermal experiments, both lithologies revealed significant increases of susceptibility around 400–500ºC preventing, in many specimens, any further identification of the NRM components. Examples of susceptibility *vs*. temperatures plots are presented in Figs 5 and 6.

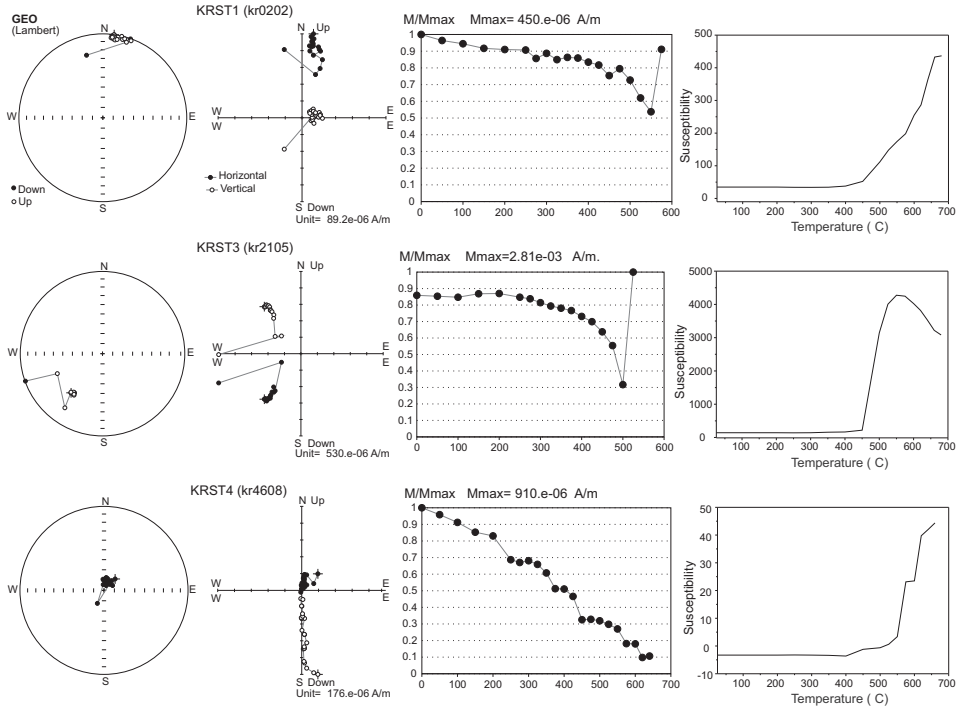

Fig. 6. Examples of thermal demagnetization and susceptibility diagrams of the red sediment fills of the karstic/tectonic fractures from Kongsfjorden; diagrams order and other explanations as in Fig. 5.

In both lithologies, up to 250ºC a low temperature less stable component (labelled L) was demagnetized that has been recorded by the recent magnetic field (Figs 5, 6 and 7A).

The metacarbonates displayed two types of thermal demagnetization patterns. In the first type, the NRM was dominated by a component that became demagnetized between 250º and 350ºC (labelled M; Figs 5 and 7B), which is most likely to be carried by pyrrhotyte, as is suggested by the Lowrie test (Fig. 4). In the second type, ferromagnetic carriers became demagnetized by 575ºC (Figs 5 and 7C). Demagnetization of these grains actually took place over a wide range of temperatures between 250ºC and 575ºC, which have been labelled component MH. Other grains, which became demagnetized in the final stages of demagnetization above 350ºC, are labelled component H.

For the fracture fills, one NRM pattern prevailed with one dominant direction, which became demagnetized by 680ºC (Figs 6 and 7C), carried by hematite. This component, which was demagnetized in the majority of cases, in the broad 250–680ºC range of temperatures, is labelled component MH. Only in site KRST1, that direction was demagnetized above 350ºC and was labelled H (Figs 6 and 7C).

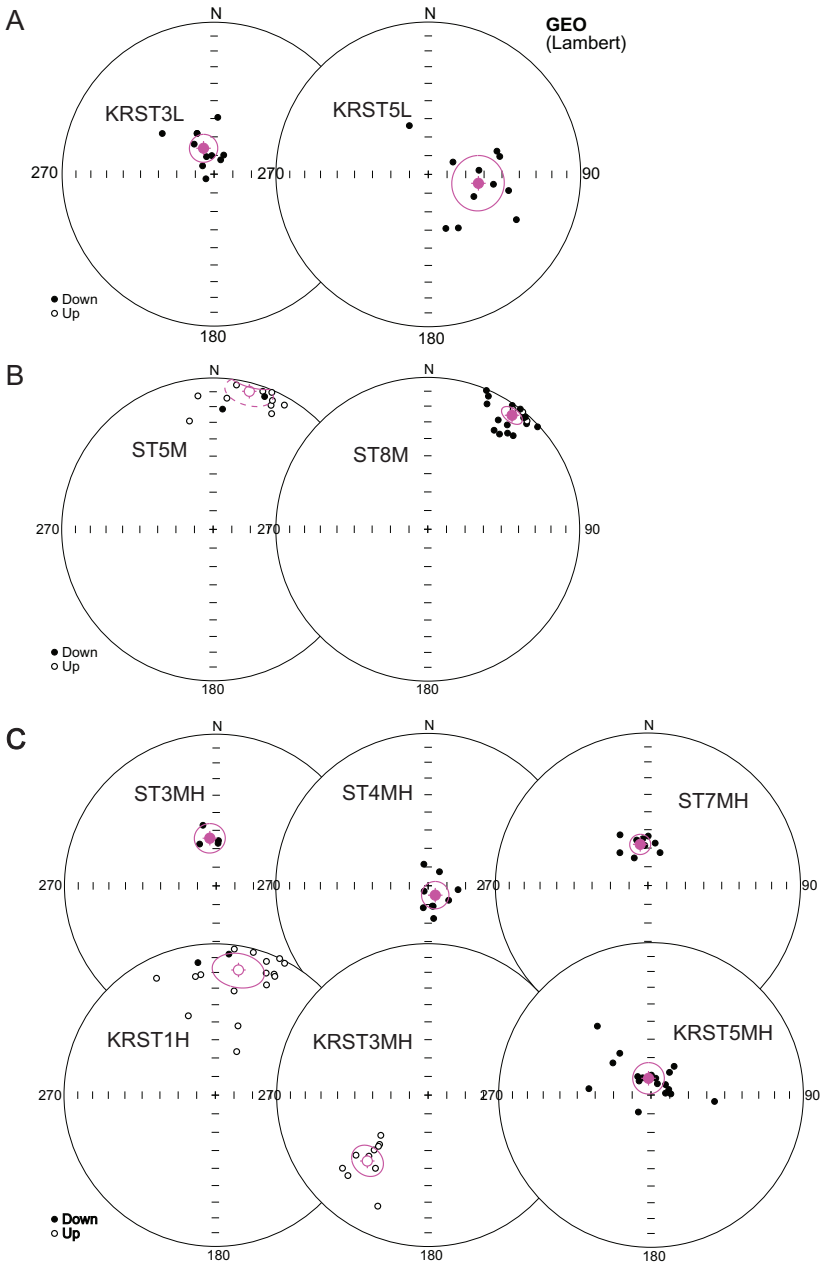

Fig. 7. Equal area projections of palaeomagnetic directions that qualified for further palaeogeographical – tectonic interpretation: (**A**) – L T_{ub} components; (**B**) – M T_{ub} components; (**C**) – MH-H T_{ub} components; all directions are presented for *in situ* orientation; site means are presented with their cones of the confidence limit α95; statistical parameters of presented components are given in Table 1; open symbols represent upper hemisphere and filled symbols represent lower hemisphere.

It should be noted that 4 of 13 sites were rejected from final interpretation (Table 1) as their site means did not pass the modified criterion of Van der Voo (1993) – $\kappa > 10$, $\alpha 95 < 16°$. Three of the metacarbonate sites (sites ST1, 2 and 6) and one site representing the brecciated fracture infilling composed of fragments of adjacent metacarbonates (site KRST2) were rejected. The scattering of directions in particular sites can be partly explained by the overlapping of the temperature spectra and incomplete cleaning of particular components. In some cases, the failure of the experiment can be the result of the relatively low signal of specimens approaching noise level of SQUID (5 μA/m) and/or by mineralogical changes which appear during the course of thermal demagnetization and disturb the initial NRM pattern.

Discussion

In any of investigated sites, the maximum low field AMS axes – K1 were not parallel to qualified palaeomagnetic directions (Supplementary material). That suggests that qualified NRM components were not modified tectonically. In metacarbonates from sites ST1 and ST8, K3 minimum AMS axes are precisely defined (half-angles of the principal diameters of the 95% confidence K3 AMS ellipses below 15º) and K1–K2 axes planes are parallel to metamorphic schistosity. In fractures infillings at sites KRST1 and KRST2, weakly developed AMS foliation can reflect bedding (half-angles of the principal diameters of the 95% confidence K3 AMS ellipses are as follows: KRST1 – 21.4º/16.1º and KRST2 – 40.4º/14º).

None of the Virtual Geomagnetic Poles (VGP's), calculated according to the components identified in the Kongsfjorden metacarbonates, fit the Proterozoic – Lower Paleozoic (pre-Silurian) sectors of the reference path, which suggests complete remagnetization of these rocks (Table 2 and Fig. 8). Components ST5M and ST8M, which became demagnetized by 350ºC, are most probably carried by pyrrhotite, which has been shown to be a common metamorphic ferromagnetic mineral in the Caledonian basement of Svalbard (*e.g.*, Michalski *et al*. 2012, 2014, 2017). The VGP's calculated according to ST5M and ST8M components in their *in situ* orientation (Table 2 and Fig. 8) fall into Caledonian *sensu lato*/ Svalbardian? sector of the Baltica/Laurussia reference (450–340 Ma) path thus assigning the deformation of Blomstrandhalvøya and Lovénøyane basement rocks mainly to the Caledonian tectono-genesis. This is demonstrable especially in the Lovénøyane site (ST8), where the basement is characterized by intensive F2 folding (the orientation of schistosity in site ST8 – 106/80; F2 fold axis 021/40 – Manby, personal communication) and the VGP calculated according to *in situ* (post-folding) orientation of the ST8M component falls exactly into 420 Ma/370–340 Ma sector of the reference APWP (Fig. 8). After tectonic correction

Table 1

Orientations and statistical parameters of palaeomagnetic directions identified in metacarbonates (sites ST1-9) and red sediments infilling the karstic/tectonic fractures (sites KRST1-4) from Blomstrandhalvøya and Lovènøyane (Kongsfjorden). Abbreviations: D – declination, I – inclination, S – total number of independently oriented hand samples collected and subjected to demagnetization procedures, s – total number of demagnetized cylindrical specimens, N/n – number of independently oriented hand samples/cylindrical specimens used for Fisher statistics, α95 – half angle of a cone of the confidence limit α95, κ – Fisherian precision parameter; all components are presented for an *in situ* orientation; components characterized by α95 > 90° and/or N < 3 are not shown in the table; grey shaded are components that qualified for further tectonic interpretation (κ>10, α95 < 16°, min. N=3).

Site	Component	D (°)	I (°)	S/s	N/n	α95	κ
ST1	ST1L	65.7	22.0	7/17	5/7	21.5	8.86
ST2	ST2M	246.6	36.4	6/18	3/3	34.0	14.23
ST3	ST3L	301.8	66.8	7/18	5/9	19.8	7.74
	ST3M	175.9	7.0	7/18	4/6	141.3	1.22
	ST3MH	352.4	64.1	7/18	¾	8.1	130.68
ST4	ST4H	142.9	83.7	6/18	6/9	7.3	50.92
ST5	ST5M	14.7	-6.4	6/18	6/12	9.9	20.27
ST6	ST6L	36.3	67.7	7/18	7/12	21.6	5.01
	ST6M	52.5	7.6	7/18	5/8	54.5	1.99
ST7	ST7L	50.2	51.7	7/18	3/3	64.6	4.72
	ST7MH	349.4	67.6	7/18	3/9	5.5	89.75
ST8	ST8M	36.5	7.4	7/18	7/18	4.8	53.19
ST9	–	–	–	6/13	–	–	–
KRST1	KRST1L	63.8	65.7	9/19	8/14	17.6	6.05
	KRST1H	10.5	-17.0	9/19	9/18	11.4	10.24
KRST2	KRST2L	9.4	77.1	6/18	4/6	17.5	15.64
	KRST2M	1.4	-4.2	6/18	4/8	47.3	2.33
KRST3	KRST3L	337.9	75.1	9/20	6/11	7.5	37.93
	KRST3MH	222.7	-40.5	9/20	6/10	8.4	34.32
KRST4	KRST4L	100.1	62.7	8/20	8/11	14.4	11.05
	KRST5MH	351.6	81.0	8/20	8/18	8.4	17.97

Table 2

Palaeopoles calculated from ChRM components identified in metacarbonates and red sediments infilling karstic/tectonic fractures of Kongsfjorden (average sampling location 79°N, 12°E); index *cor* indicates palaeopoles calculated after tectonic corrections according to F2 deformations (metacarbonates) or identified AMS foliation (fracture infilling in site KRST1).
Abbreviations: P – polarity (N, normal; R, reverse); Φ – palaeopole latitude; Λ – palaeopole longitude; D_p/D_m – half-axes of palaeopole oval of the confidence limit α95; Plat – palaeolatitude; other abbreviations as in Table 1.

VGP Symbol	N	n	P	D (°)	I (°)	α95 (°)	κ	Φ (°) N	Λ (°) E	D_p/D_m (°)	Plat (°)
ST3MH	3	4	N	352.4	64.1	8.1	130.8	-56.7	21.7	10.3/12.9	45.8
ST3MHcor			N	40	65.20	47.10	4.77	-55.10	322.32	61.7/76.2	47.3
ST4H	6	9	N	142.9	83.7	7.3	50.92	-67.8	212.1	14.1/14.3	77.6
ST4Hcor			N	119.3	32.4	7.3	50.92	-12.0	250.2	4.7/8.2	17.6
ST5M	6	12	R	14.7	-6.4	9.9	20.27	-7.4	357.2	5.0/9.9	3.2
ST5Mcor			R	14.7	-6.4	9.9	20.27	-7.4	357.2	5.0/9.9	3.2
ST7MH	3	9	N	349.4	67.6	5.5	89.75	-61.3	26.1	7.7/9.2	50.5
ST7MHcor			N	37.0	25.0	5.5	89.75	-21.8	332.9	3.2/5.9	13.1
ST8M	7	18	N	36.1	7.4	4.8	53.19	-12.5	334.6	2.4/4.8	3.7
ST8Mcor				356.0	-63.0	4.8	53.19	-33.5	195.4	5.9/7.5	44.5
KRST1H	9	18	R	10.5	-17.0	11.4	10.24	-2.1	1.6	6.1/11.8	8.7
KRST1Hcor			R	36	-40	11.4	10.24	13.7	338.1	8.3/13.7	22.8
KRST3MH	6	10	R	222.7	-40.5	8.4	34.32	-31.0	325.3	6.1/10.2	23.1
KRST4MH	8	18	N	351.6	81.0	8.4	17.97	-83.1	33.6	15.7/16.2	72.4

according to the F2 folding ST8M VGP becomes distant from the reference path (Fig. 8), hence suggesting the magnetic fabric post-dates the folding.

In contrast to the M ChRM (Characteristic Remanent Magnetization), the MH and H components of the metacarbonates (ST3MH, ST4H, ST7MH) are characterized in *in situ* position by steeper inclinations (from 64° up to 83°), which suggests that they represent younger Mesozoic/Cenozoic remagnetizations (Table 2 and Fig 9). Those components are most likely carried by maghemite and, or low-Ti magnetite. The ST3MH component was identified in site ST3, which is characterized by varied orientations of the schistosity. The within-site palaeomagnetic fold test revealed a post-folding origin of the ST3MH component (Table 2), which is superimposed over F2 structures. The ST3MH *in situ*

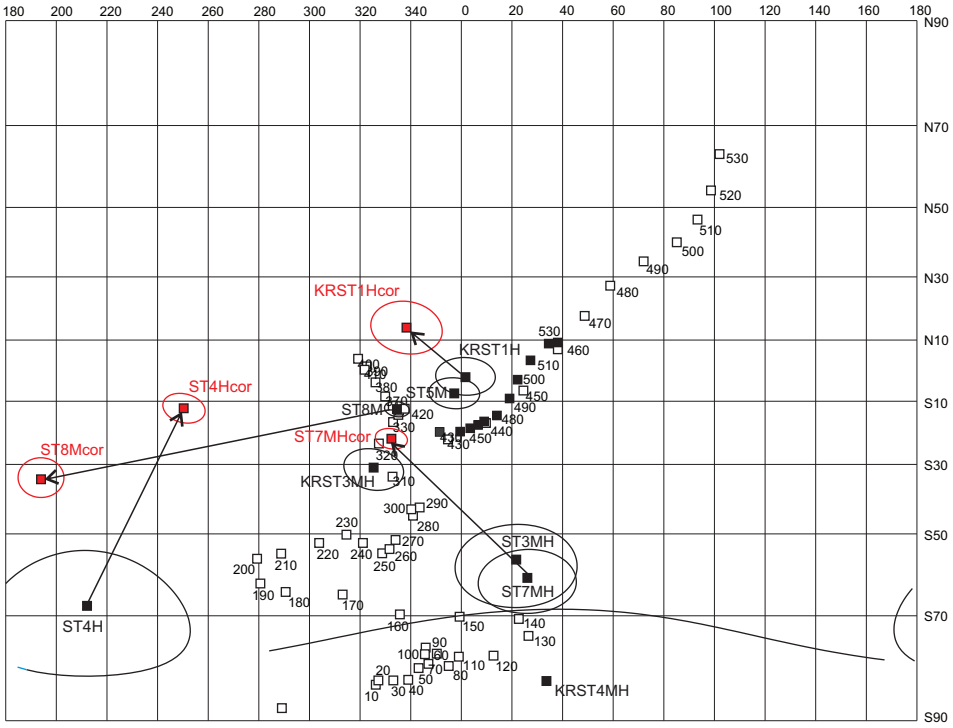

Fig. 8. Palaeopoles calculated for middle- to high-temperature components (M, H, MH) identified in Kongsfjorden (this study) with their ellipses of the confidence limit α95 against reference path of Laurussia (open squares, palaeopoles 0–430 Ma), Baltica (open squares, palaeopoles 440–530 Ma) and Laurentia (filled squares, palaeopoles 440–530 Ma); reference palaeopoles were taken from Torsvik *et al.* (2012); ages of particular palaeopoles are given; black ovals represent *in situ* palaeopoles before tectonic correction; in the case of metacarbonates grey ovals (red in on-line version) represent VGP's after tectonic corrections according to F2 deformations; as ST5 was characterized by horizontal schistosity in that site tectonic correction was not applied; in the case of KRST1 site grey oval (red in on-line version) indicates position of VGP after correction according to identified weakly developed AMS foliation; Galls projection.

VGP falls in the vicinity 130–150 Ma sector of the Laurussia APWP (Fig. 8). A similar position is occupied by the ST7MH *in situ* VGP. In this case however, unfolding of the F2 structure in site ST7 moves ST7MH palaeopole into 320–330 Ma sector of the reference path (VGP ST7MHcor, see also Table 2). This would suggest that the folding, in this particular site, could have taken place after the Caledonian/Svalbardian deformation events and that the ST7MH component represents a 330-320 Ma remagnetization. The ST4H VGP does not fit any sector of the reference path either before or after tectonic correction (Fig. 8). A very steep inclination of the *in situ* ST4H component – 83ºN (Table 2 and Fig. 9) suggests that it can be related to the youngest palaeomagnetic record

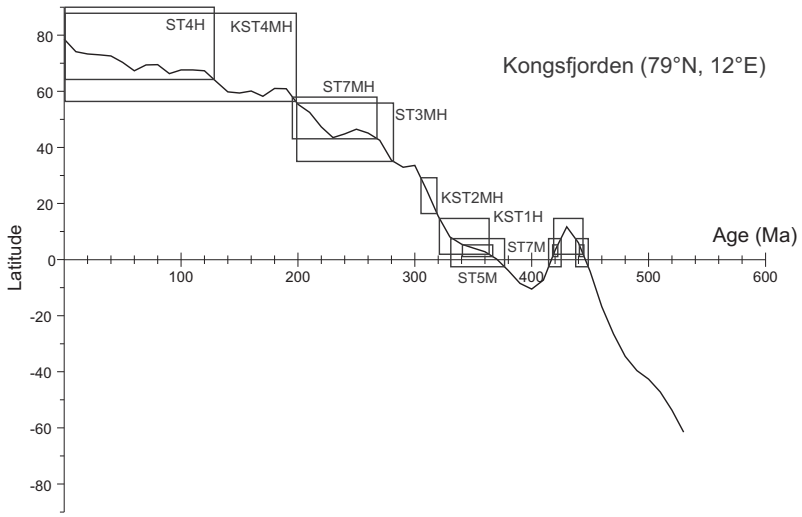

Fig. 9. Paleolatitudes of Blomstrandhalvøya and Lovénøyane during magnetization of M, H (MH) components (this study). Reference palaeolatitude curve for the Kongsfjorden sampling area (average location 78°N, 12°E) has been calculated from Laurussia (0–430 Ma) and Baltica (440–530 Ma) APWPs, derived from GMAP 2012 libraries (Torsvik *et al.* 2012). All palaeolatitudes of M, H (MH) components/VGP's of the Kongsfjorden islands are recalculated for the northern hemisphere and are presented with confidence limits defined by D_p (half-axis of palaeopole oval of the confidence limit α95).

of Kongsfjorden, *e.g.*, Palaeogene remineralization and possible remagnetization related to evolution of the WSFTB.

The VGP's calculated according to the MH – H components identified in the sediments fills of the karstic/tectonic fractures cutting metacarbonates of Blomstrandhalvøya for the *in situ* position fall into sectors of the Laurussia – Baltica reference path (Table 2 and Fig. 8) as follows: (i) Caledonian *sensu lato* (450–380 Ma) – palaeopole KRST1H; (ii) Carboniferous (320–310 Ma) – palaeopole KRST3MH, and (iii) Cretaceous – rec (150–0 Ma) – palaeopole KRST4MH. Correction in the site KRST1 according to identified weakly developed AMS foliation (Supplementary material) brings the KRST1H VGP slightly closer to the 390–410 Ma sector of the APWP (Table 2 and Fig. 8). The first two ages can be related to deposition of the sampled sediments: (i) directly after Caledonian tectonism, during the Late Silurian/ Devonian collapse of the Caledonian orogen that led to the unroofing and karstification of the metamorphosed Caledonian complexes (Braathen *et al*. 2018), and (ii) in Carboniferous time during the first of the Barents Sea rifting phases defined by Clark *et al*. (2014). The second age is in accordance with Buggisch *et al*. (1994) who from

conodont fauna assigned a Middle Carboniferous age of one of the cavity fills. Accordingly, they postulate that karstification for that site must have taken place in Early Carboniferous time or earlier. It should be noted also that *in situ* LA-ICP-MS $^{40}Ar/^{39}Ar$ age determinations in the adjacent metamorphic complexes of Ossian Sarsfjellet and Brøggerhalvøya, provide evidence for the occurrence of three thermal events, during the 426–380 Ma Caledonian (*sensu lato*) metamorphism, and the 377–326 Ma and *ca*. 300 Ma intervals (Michalski *et al*. 2017). These events could have influenced the palaeomagnetic record of the Kongsfjorden area. The KARST4MH component, which is characterized by the steep inclination, could be related to the Late Mesozoic extension and injection of dolerite dikes (*e.g*., Nejbert *et al*. 2011; Polteau *et al*. 2016) or the Eurekan tectonogenesis (*e.g*., Lyberis and Manby 1993; Maher *et al*. 1995).

The coincidence of the majority of the VGP's calculated for the components identified in both of the sampled lithologies, with the reference Laurussia path from 430 Ma, suggests that the geometry of the basement on Blomstrandhalvøya and Lovénøyane has not been significantly modified since Late Caledonian time. During the formation of the WSFTB the studied area may have been located in front of or, alternatively, overridden by the Eurekan thrust sheets found in adjacent Brøggerhalvøya area (*e.g*., Bergh *et al*. 2000; Saalmann and Thiedig 2001, 2002). It should be noted, however, that on the basis of the palaeomagnetic data presented here, post-magnetization rotations cannot be completely ruled out. Firstly, the NRM components that qualified for the final tectonic interpretation were calculated with a defined precision ($\alpha 95$ from 4.8° to 11.4°; Table 1). Furthermore, the imprecise fit of the selected VGP's (*e.g*., KRST1H) with the reference path may be related to local tilting of the sediments fills following reactivation of the fault zone.

To the south of Kongsfjorden, the adjacent western margin of Oscar II Land has been interpreted to have been affected by *ca*. 40° eastward tilting of the basement blocks along west-dipping NNW–SSE trending listric normal faults related to the early stage of opening of the North Atlantic Ocean (Michalski *et al*. 2017). The application of similar corrections to the data for the basement rocks of Blomstrandhalvøya and Lovénøyane do not provide any evidence for fault related tilting (Fig. 10). Applying a listric fault tilt-correction to the VGP's does produce a better fit to the reference path for some palaeopoles (*e.g*., ST3MH, ST7MH), however, the majority move further from the APWP (*e.g*., ST8M).

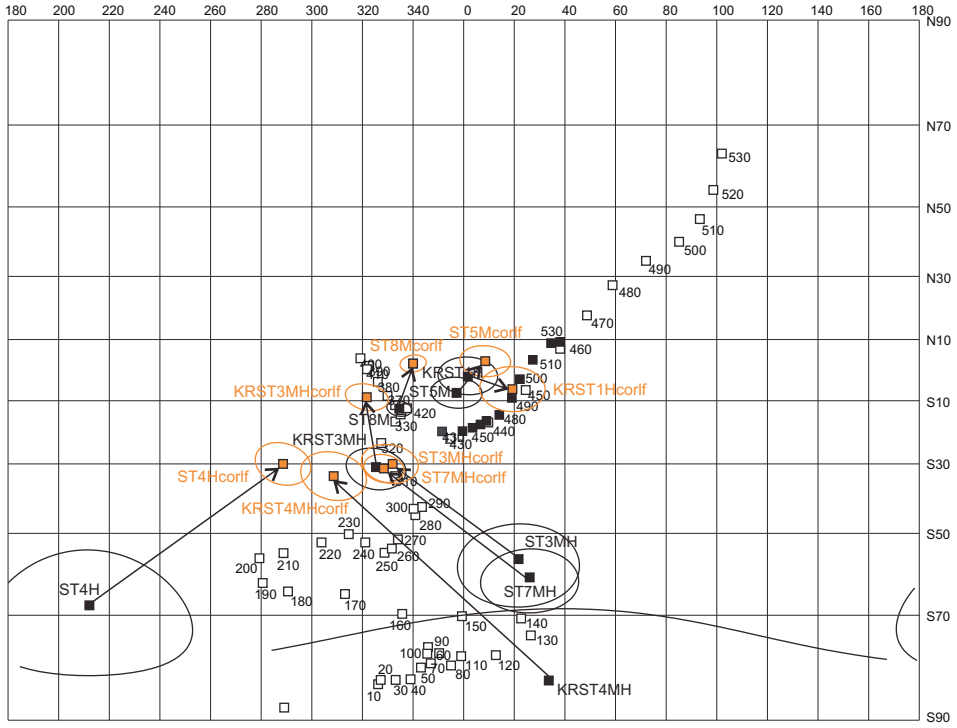

Fig. 10. Palaeopoles calculated for middle to high-temperature components (M, H, MH) identified in Kongsfjorden (this study) against reference path of Laurussia (palaeopoles 0–430 Ma), Baltica (palaeopoles 440–530 Ma) and Laurentia (palaeopoles 440–530 Ma); black ovals represent position of palaeopoles before, and grey ovals (orange in on-line version) represent positions after tectonic corrections according to west-dipping listric normal faults rotations (rotation around horizontal axis N 160°, by the angle 40°); Galls projection; other explanations as in Fig. 8.

Conclusions

1. The palaeomagnetic investigation of metacarbonates from Blomstrandhalvøya and Lovénøyane described in this contribution do not indicate the preservation of any pre-metamorphic palaeomagnetic record in the Kongsfjorden basement. The data obtained does indicate, however, Caledonian *sensu lato*/Svalbardian? and Late Mesozoic/Cenozoic remagnetization events, which are carried by the pyrrhotite and magnetite/maghemite phases, respectively.
2. The palaeomagnetic experiments conducted on the unmetamorphosed red sediments infilling the karstic/tectonic fractures within the metamorphic basement on Blomstrandhalvøya reveal that the sediments could have been deposited and/or remagnetized in the Caledonian *sensu lato*, Carboniferous and Late Mesozoic/Cenozoic intervals. Fracturing and karstification of

Kongsfjorden area has been confirmed to have taken place in early Devonian to Carboniferous time, or even in Late Silurian time, following the collapse and unroofing of the Caledonian Orogen.

3. The palaeomagnetic results from the basement on Blomstrandhalvøya and Lovénøyane attribute the origin of the F2 folds in metacarbonates to Caledonian/Svalbardian tectono-genesis. As the majority of the palaeopoles calculated for the Kongsfjorden samples fit the Laurussia reference path in an *in situ* orientation, these results support the hypothesis (*e.g.*, Thiedig *et al*. 2001) that Kongsfjorden islands escaped main Eurekan deformation.
4. This study does not confirm the modification of the Kongsfjorden basement geometry by any west dipping listric fault activity accompanying the opening of North Atlantic Ocean of the kind postulated by Michalski *et al*. (2017) for the adjacent Forlandsundet/Oscar II Land area to the south.
5. Without doubt more palaeomagnetic analyses are needed to fully describe and understand sequence of tectono-thermal processes that have influenced Caledonian metamorphic basement of the Kongsfjorden area.

Acknowledgements. — This study is part of the PALMAG project 2012–2016: *Integration of palaeomagnetic, isotopic and structural data to understand Svalbard Caledonian Terranes assemblage* funded by Polish National Science Centre (NSC) – grant number 2011/03/D/ST10/05193. Preliminary palaeomagnetic samples for this study were collected in 2006 in the course of the joint expedition of the Institute of Geophysics, Polish Academy of Sciences and University of Greenwich (United Kingdom) that was carried out along the western and the northern margins of Spitsbergen (Oscar II Land, Forlandsundet, Kongsfjorden, Sorgfjorden). The main palaeomagnetic sampling were undertaken in 2012 in the course of the palaeomagnetic expedition to Western Oscar II Land (St. Jonsfjorden and Engelskbukta) and Kongsfjorden (Brøggerhalvøya and Blomstrandhalvøya) funded by the Polish NSC. I am deeply grateful to Geoffrey Manby for his conceptual and linguistic improvements of the manuscript and to Aleksandra Hołda Michalska for redrawing the geological map of Kongsfjorden and improvements of the figures. I would also like to express my gratitude to Alvar Braathen and Jerzy Nawrocki for their profound and valuable reviews.

References

Bergh S.G., Braathen A. and Andresen A. 1997. Interaction of basement-involved and thin-skinned tectonism in the Tertiary Fold-Thrust Belt of Central Spitsbergen, Svalbard. *AAPG Bulletin* 81: 637–661.

Bergh S.G., Maher H.D. and Braathen A. 2000. Tertiary divergent thrust directions from partitioned transpression, Brøggerhalvøya, Spitsbergen. *Norsk Geologisk Tidsskrift* 80: 63–81.

Bergh S.G., Maher H.D. and Braathen A. 2011. Late Devonian transpressional tectonics in Spitsbergen, Svalbard, and implications for basement uplift of the Sørkapp –Hornsund High. *Journal of the Geological Society* 168: 441–456.

BRAATHEN A., BERGH S.G. and MAHER H.D. Jr. 1999. Application of a critical wedge taper model to the Tertiary transpressional fold-thrust belt on Spitsbergen, Svalbard. *GSA Bulletin* 111: 1468–1485.

BRAATHEN A., OSMUNDSEN P.T., MAHER H. and GANERØD M. 2018. The Keisarhjelmen detachment records Silurian–Devonian extensional collapse in Northern Svalbard. *Terra* 30: 34–39.

BUGGISH W., PIEPJOHN K., THIEDIG F. and GOSEN W. von. 1994. A Middle Carboniferous conodont fauna from Blomstrandhalvøya (NW Spitsbergen). Implications on the age of post-Devonian karstification and Svalbardian deformation. *Polarforschung* 62: 83–90.

BURZYŃSKI M., MICHALSKI K., NEJBERT K., DOMAŃSKA-SIUDA J. and MANBY G. 2017. High-resolution mineralogical and rock magnetic study of ferromagnetic phases in metabasites from Oscar II Land, Western Spitsbergen—towards reliable model linking mineralogical and palaeomagnetic data. *Geophysical Journal International* 210: 390–405.

CHADIMA M. and HROUDA F. 2009. Remasoft 3.0: Paleomagnetic data browser and analyzer. Agico, Inc. Brno, Czech Republic (www.agico.com).

CHADIMA M. and JELINEK V. 2009. AniSoft 42 Software, anisotropy data browser for Windows. Agico, Inc. Brno, Czech Republic (www.agico.com).

CLARK S.A., GLORSTAD-CLARK E., FALEIDE J.I., SCHMID D., HARTZ E.H. and FJELDSKAAR W. 2014. Southwest Barents Sea rift basin evolution: comparing results from backstripping and time forward modelling. *Basin Research* 26: 550–566.

DEKKERS, M.J. 1988. Magnetic properties of natural pyrrhotite part 1: behavior of initial susceptibility and saturation-magnetization related parameters in a grain-size dependent framework. *Physics of the Earth and Planetary Interiors* 52: 376–393.

DUNLOP D.J. and ÖZDEMIR Ö. 1997. *Rock magnetism fundamentals and frontiers*. Cambridge University Press, Cambridge: 573 pp.

FISHER R.A. 1953. Dispersion on a sphere. *Proceedings of the Royal Society of London* 217: 295–305.

FRIEND P.F. 1961. The Devonian stratigraphy of North and Central Vestspitsbergen. *Proceedings of the Yorkshire Geological Society* 33: 77–118.

GEE D.G. and HJELLE A. 1966. On the Crystalline Rocks of Northwest Spitsbergen. *Norsk Polarinstitutt* Årbok. 1964: 31–45.

HARLAND W.B. and WRIGHT N. 1979. Alternative hypothesis for the pre-Carboniferous evolution of Svalbard. *Norsk Polarinstitutt Skrifter* 167: 89–117.

HJELLE A. 1979. Aspects of the geology of Northwest Spitsbergen. *Norsk Polarinstitutt Skrifter* 167: 37–62.

HJELLE A., PIEPJOHN K., SAALMANN K., OHTA Y., SALVIGSEN O., THIEDIG F. and DALLMANN W. 1999. Geological map of Svalbard 1:100 000, sheet A7G Kongsfjorden. Norsk Polarinstitutt Temakart No. 30.

JELINEK V. 1981. Characterization of the magnetic fabric of rocks. *Tectonophysics* 79: 63–67.

KEMPE M., NIEHOFF U., PIEPJOHN K. and THIEDIG F. 1997. Kaledonische und svalbardische Entwiclung im Grundgebirge auf der Blomstrandhalvøya, NW-Spitzbergen. *Münstersche Forschungen zur Geologie und Paläontologie* 82: 121–128.

KIRSCHVINK J. 1980. The least square line and plane and analysis of paleomagnetic data. *Geophysical Journal of the Royal Astronomical Society* 62: 699–718.

LEEVER K.A., GABRIELSEN R.H., FALEIDE J.I. and BRAATHEN A. 2011. A transpressional origin for the West Spitsbergen fold-and thrust belt: insight from analog modeling. *Tectonics* 30: 1–24.

LYBERIS N. and MANBY G.M. 1993. The origin of the West Spitsbergen Fold Belt from geological constraints and plate kinematics: implications for the Arctic. *Tectonophysics* 224: 371–391.

LOWRIE W. 1990. Identification of ferromagnetic minerals in a rock by coercivity and unblocking

temperature properties. *Geophysical Research Letters* 17: 159–62.

MAHER H.D., BRAATHEN A., BERGH S., DALLMANN W. and HARLAND W.B. 1995. Tertiary or Cretaceous age for Spitsbergen's fold-thrust belt on the Barents Shelf. *Tectonics* 14: 1321–1326.

MANBY G. and LYBERIS N. 1992. Tectonic evolution of the Devonian Basin of northern Svalbard. *Norsk Geologisk Tidsskrift* 72: 7–19.

MICHALSKI K., LEWANDOWSKI M. and MANBY G.M. 2012. New palaeomagnetic, petrographic and $^{40}Ar/^{39}Ar$ data to test palaeogeographic reconstructions of Caledonide Svalbard. *Geological Magazine* 149: 696–721.

MICHALSKI K., NEJBERT K., DOMAŃSKA-SIUDA J. and MANBY G. 2014. New palaeomagnetic data from metamorphosed carbonates of Western Spitsbergen, Oscar II Land. *Polish Polar Research* 35: 553–592.

MICHALSKI K., MANBY G., NEJBERT K., DOMAŃSKA-SIUDA J. and BURZYŃSKI M. 2017. Using palaeomagnetic and isotopic data to investigate late to post-Caledonian tectonothermal processes within the Western Terrane of Svalbard. *Journal of the Geological Society* 174: 572–590.

NEJBERT K., KRAJEWSKI K.P., DUBIŃSKA E. and PÉCSKAY Z. 2011. Dolerites of Svalbard, north-west Barents Sea Shelf: age, tectonic setting and significance for geotectonic interpretation of the High-Arctic Large Igneous Province. *Polar Research* 30: 7306.

PIEPJOHN K., VON GOSEN W. and TESSENSOHN F. 2016. The Eurekan deformation in the Arctic: an outline. *Journal of the Geological Society* 173: 1007–1024.

POLTEAU S., HENDRIKS B.W.H., PLANKE S., GANERØD M., CORFU F., FALEIDE J.I., MIDTKANDAL I., SVENSEN H. and MYKLEBUST R. 2016. The Early Cretaceous Barents Sea sill complex: Distribution, $^{40}Ar/^{39}Ar$ geochronology, and implications for carbon gas formation. *Palaeogeography, Palaeoclimatology, Palaeoecology* 441: 83–95.

THIEDIG F. and MANBY G.M. 1992. Origins and deformation of post-Caledonian sediments on Blomstrandhalvøya and Lovénøyane, Northwest Spitsbergen. *Norsk Geologisk Tidsskrift* 72: 27–33.

THIEDIG F., SAALMANN K. and PIEPJOHN K. 2001. Explanatory notes to the geological map of Brøggerhalvøya and Blomstrandhalvøya 1:40,000. *In*: Tessensohn F. (ed.) Intra-continental fold belts. Case 1: West Spitsbergen. *Geologisches Jahrbuch Reihe* B 91: 25–51.

TORSVIK T.H., VAN DER VOO R., PREEDEN U., MAC NIOCAILL C., STEINBERGER B., DOUBROVINE P.V., VAN HINSBERGEN D.J.J., DOMEIER M., GAINA C., TOHVER E., MEERT J.G., MCCAUSLAND P.J.A. and COCKS L.R.M. 2012. Phanerozoic polar wander, paleogeography and dynamics. *Earth-Science Reviews* 114: 325–368.

SAALMANN K. and THIEDIG F. 2001. Tertiary West Spitsbergen fold and thrust belt on Brøggerhalvøya, Svalbard: Structural evolution and kinematics. *Tectonics* 20: 976–998.

SAALMANN K. and THIEDIG F. 2002. Thrust tectonics on Brøggerhalvøya and their relationship to Tertiary West Spitsbergen Fold-and-Thrust Belt. *Geological Magazine* 139: 47–72.

SZLACHTA K., MICHALSKI K., BRZÓZKA K., GÓRKA B. and GAŁĄZKA-FRIEDMAN J. 2008. Comparison of magnetic and Mössbauer results obtained for Palaeozoic rocks of Hornsund, Southern Spitsbergen, Arctic. *Acta Physica Polonica* A 114 (6): 1675–1682.

VAN DER VOO R. 1993. *Paleomagnetism of the Atlantic, Tethys and Iapetus Oceans*. Cambridge University Press, Cambridge: 411 pp.

Received 22 November 2017
Accepted 15 January 2018

Supplementary material: Anisotropy of magnetic susceptibility

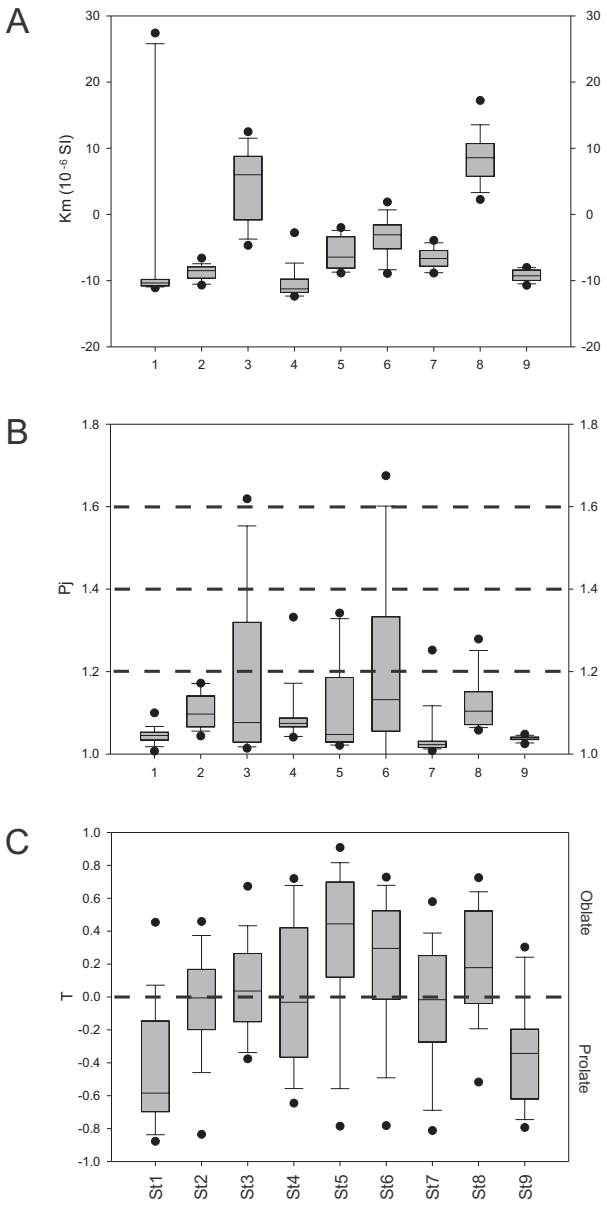

Fig. SM1. Low field anisotropy of magnetic susceptibility (AMS) of metacarbonates of Blomstrand and Lovèn islands (Kongsfjord); (**A**–**C**) box and whisker plots presenting distribution of (**A**) mean susceptibility (Km), (**B**) corrected anisotropy degree sensu Jelinek (1981) – Pj, (**C**) shape parameter (T) in the following palaeomagnetic sites of metacarbonates (ST1-9); 25% and 75%

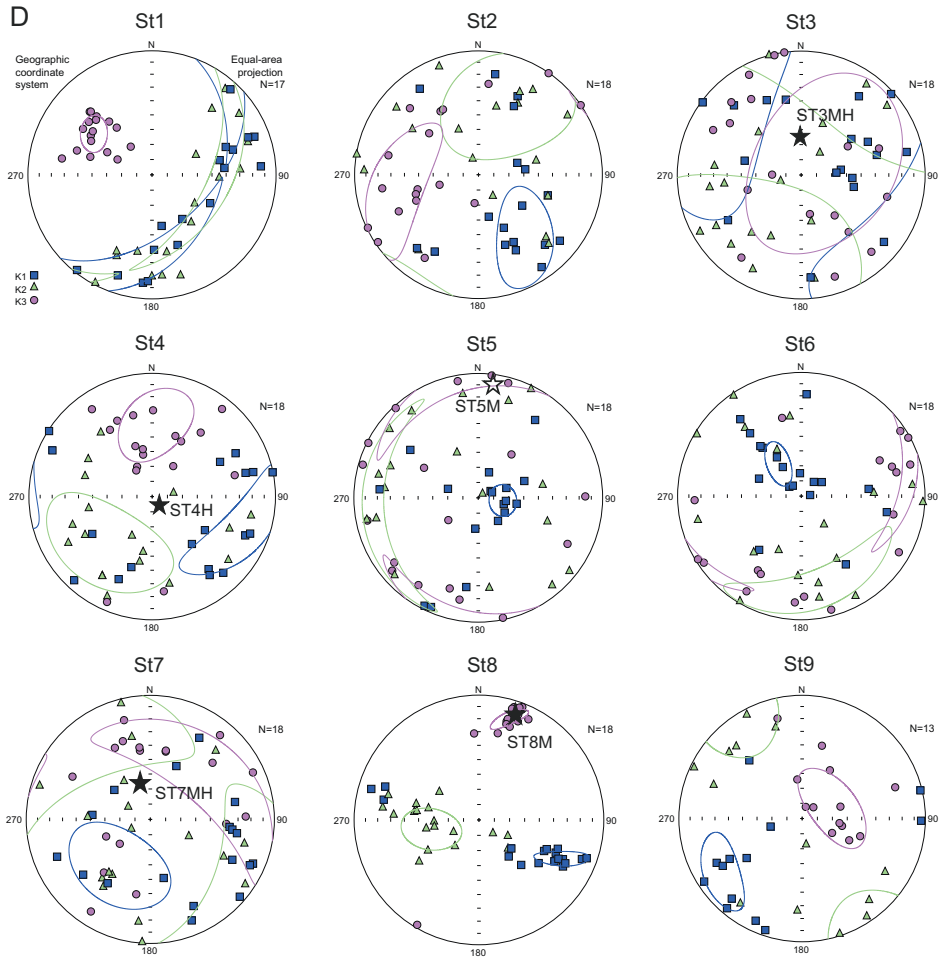

percentiles are shown by boxes, the mean value is given by horizontal line inside boxes, 10% and 90% percentiles are presented by whiskers, minimum and maximum values are marked by dots; (**D**) distribution of AMS principal axes in palaeomagnetic sites of metacarbonates; squares, triangles, circles represent K1 (max), K2 (intermediate) and K3 (min) principal axes of AMS respectively; confidence ellipses of particular axes are presented; names of the sites are given; orientations of palaeomagnetic components qualified for tectonic interpretation are marked by stars; filled symbols – lower hemisphere, open symbols – upper hemisphere; equal area projections.

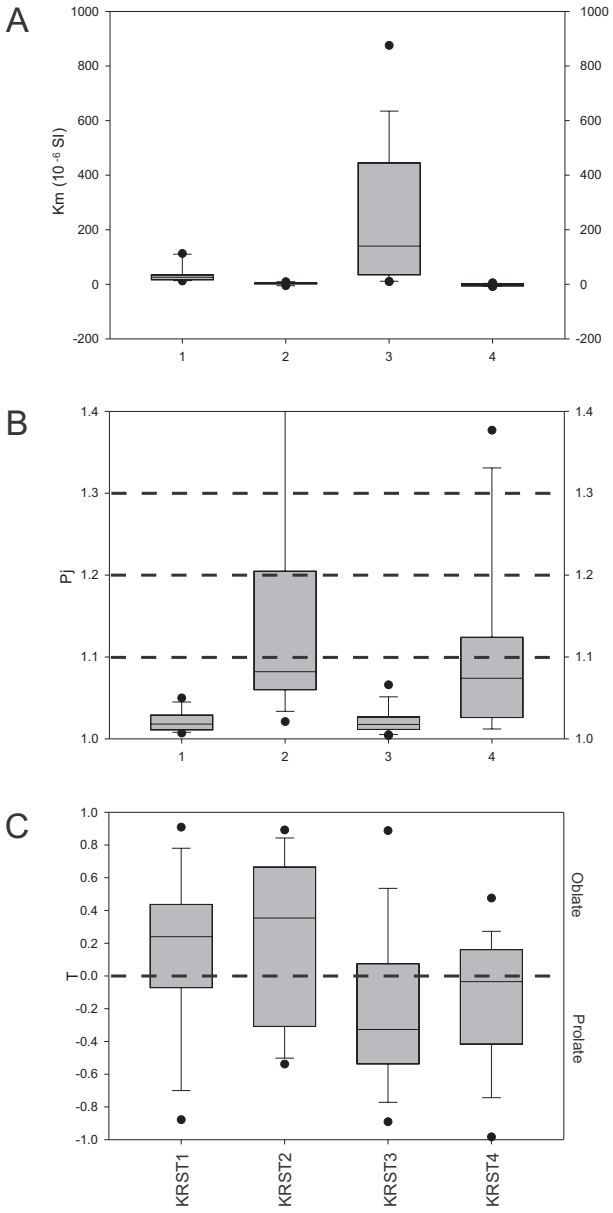

Fig. SM2. Low field anisotropy of magnetic susceptibility (AMS) of the sediments infilling fractures in Blomstrand island (Kongsfjord); (**A**–**C**) box and whisker plots presenting distribution of (**A**) mean susceptibility (Km), (**B**) corrected anisotropy degree sensu Jelinek (1981) – Pj,

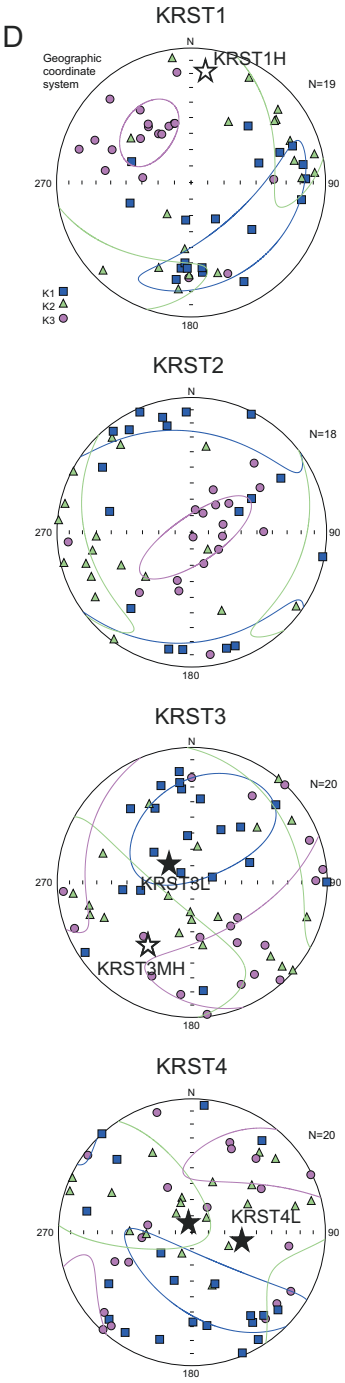

(**C**) shape parameter (T); (**D**) distribution of AMS principal axes in palaeomagnetic KRST1–4; other abbreviations are as in Fig. SM1.